Journal of Materials Chemistry B

Accepted Manuscript

ROYAL SOCIETY OF CHEMISTRY

www.rsc.org/materialsB

Journal of Materials Chemistry B

ARTICLE

Layered Polymeric Capsules Inhibiting Activity of RNases for Intracellular Delivery of Messenger RNA

Received 00th January 20xx,
Accepted 00th January 20xx

DOI: 10.1039/x0xx00000x

www.rsc.org/

Mitali Kakran,[a†] Masafumi Muratani,[b†‡] Weiquan John Tng,[b] Hongqing Liang,[b] Daria B. Trushina,[a, c] Gleb B. Sukhorukov,[a, d] Huck Hui Ng[b] and Maria N. Antipina*[a]

Intracellular delivery of messenger RNA (mRNA) is a promising approach for experimental and therapeutic manipulation of cellular activity. However, environmental RNase hinders reliable handling of mRNA for experimental and therapeutic use. In this study, biodegradable capsules composed of dextran sulfate and poly-L-arginine in the Layer-by-Layer (LbL) fashion are employed for protection and delivery of mRNA. Our results demonstrate that addition of RNase inhibitor to mRNA while co-precipitation with $CaCO_3$ and subsequent LbL encapsulation are both crucial to preserve integrity of mRNA. Expression of functional luciferase enzyme in HEK293T human embryonic kidney cells after incubation with synthetic luciferase-encoding mRNA capsules indicates reliability of the encapsulating system and cellular intake of functional mRNAs. These improvements in mRNA encapsulation should provide essential basis for microcapsule-based mRNA delivery for further applications.

1. Introduction

Intracellular delivery of nucleic acid is a critical process for manipulation of cellular activity in a broad range of applications. Perhaps the most striking demonstration in the field of regenerative medicine is production of induced pluripotent stem cells (iPS cells) by introduction of DNA encoding the key gene products into somatic cells.[1] Numerous studies have also supported gene delivery as a promising therapeutic strategy in human disease including Parkinson's disease, cardiovascular disorders and lysosomal disorders.[2-4] To realize more efficient and safer manipulation of cellular activity, significant efforts have been made to improve both the design of nucleic acid and delivery methods. One of the widely-used nucleic acid delivery methods is a replication-deficient viral vector. This nature-mimicking transfection method enables high efficiency and long-term gene expression[5] but has issues with immunogenicity, carcinogenicity, poor target cell specificity, inability to transfer large size genes and high costs.[6] Conventionally used non-viral transfection technologies involve three major groups of physical, electrical and chemical methods. The advantages and drawbacks of each approach extensively reviewed elsewhere[7] allow to distinguish cationic liposome mediated gene transfer as the simplest, and the least toxic method. From the prospective of cell integrity, liposomal technology also appears as one of the safest approaches. Being packed inside liposomes, the therapeutic gene sequences in their turn become protected from acidic environment of endosomes and nuclease activity. Currently available cationic lipid-based delivery (lipoplexes) or cationic polymer complexes of DNA or RNA (polyplexes) are, however, often highly toxic for the cells or not efficient for many cell types.[8-11] In addition, lipoplexes generally suffer from structural instability upon storage and exposure to blood plasma proteins, and, as such, having a shortcoming for drug manufacturing and limited administration pathways *in vivo*. This has encouraged researchers to focus on alternative materials and packaging systems, such as novel cationic lipids,[12] polymers,[13] polyhedral oligomeric silsesquioxanes,[14] nanotubes[15, 16] and graphene-based nanocomposite materials.[17, 18] Layer-by-Layer (LbL) assembled polymer capsules can offer much higher capacity for molecular cargo than liposomes, and can house multiple types of therapeutic molecules in a single entity. Given the fact that some polymer pairs can degrade inside the leaving cells by lysosomal enzymes[19] or disassemble in response to various external stimuli,[20-22] LbL capsules have been considered as perspective non-viral vectors for gene delivery. A large number of

[a] Institute of Materials Research and Engineering, A*STAR, Singapore, 117602, Singapore, 3 Research Link. Tel: +6568741974; E-mail: antipinam@imre.a-star.edu.sg (M. N. Antipina).
[b] Genome Institute of Singapore, A*STAR, Singapore, 138672 Singapore, 60 Biopolis St.
[c] Faculty of Physics M. V. Lomonosov Moscow State University, Moscow 119991 Leninskie Gory, Russia.
[d] School of Engineering and Materials Science, Queen Mary University of London, Mile End Road, London E1 4NS, United Kingdom.
† These authors equally contributed to this manuscript.
‡ M. Muratani current address: Department of Genome Biology, Faculty of Medicine, University of Tsukuba, 1-1-1 Tennodai, Tsukuba, Ibaraki 305-8575, Japan.

publications reports on incorporation of nucleic acids in nano-sized multilayer assemblies by using them as an anionic constituent of the shells formed over inorganic templates, i.e., gold[23-26] or silica[27, 28] nanoparticles, gold nanorods,[29] carbonate nanocrystals,[30] and halloysites.[31] This design has clear advantages such as the possibility of tuning the particle size in the sub-micron range and a good control over the amount of nucleic acid. Gene sequences are protected in the assembly by complementary compounds and not subjected to any further potentially harmful treatment. Biological effect of these gene-packing LbL assemblies on inorganic particle template has been reviled based on expression of the encoded proteins, and some systems have even shown considerably higher delivery efficiency compare to those available in the market.[25] An important disadvantage of this approach is the presence of inorganic template non-degradable after cell internalization. Thus, *in vivo* applications of the nanoparticle-based gene delivery systems can be limited. In a more favorable design, nucleic acids are packed inside a soft polymer multilayer shell by a multistep procedure which involves i) adsorption by a sacrificial particle template, ii) LbL shell assembly, and iii) decomposition of template. Pre-loading of double stranded DNA (dsDNA)[32] and aptamers[33] in sacrificial porous $CaCO_3$ microparticles has been reported. Another type of inorganic soluble template, amine-functionalized mesoporous silica, was used for encapsulation of oligonucleotides, linear dsDNA, plasmid DNA, and small interfering RNA (siRNA).[34-36] Since the pH conditions upon dissolution of both $CaCO_3$ and silica templates can be harmful for the encapsulated genes, there's a question mark over the gene expression activity of the payload, although gel electrophoresis has confirmed identity of encapsulated and non-encapsulated molecules.[35]

Gene delivery by introduction of exogenous DNA molecules that integrate into the genomic DNA causes unintended genetic alterations and potentially cancer-inducing mutations. Delivery of RNA molecules into the cell allows direct modulation of cellular activity by transient control of protein expression without introduction of genetic changes. In the area of stem cell research it was also confirmed that RNAs (instead of DNA) can reprogram somatic cells.[37] Commercially available RNA vectors are still at their infancy and much less effective than retroviruses. Thus, efficient and simple delivery systems specifically for RNA are highly demanded.

Comparing to packing and delivery of DNA, fabrication of RNA vectors represent an extra challenge because of the wide presence of ribonucleases (RNases) results in very short lifespans for any RNA molecule that is not in a protected environment. Exogenous RNases widely present at ambient space as a first defense of living organisms against RNA viruses can degrade the therapeutic RNA already in the stage of fabrication of the delivery vector. For removing exogenous RNase contamination, powerful RNase inhibitors have to be therefore incorporated in the fabrication process. In the present study, we elaborate $CaCO_3$ microparticle-assistant preloading method for encapsulation of RNA. A significant advantage of using $CaCO_3$ as a sacrificial template is a possibility to co-precipitate multiple types of molecules in the same particle, so that a resulting LbL assembled capsule actually carries a molecular cocktail. In such a way, basic fibroblast growth factor was encapsulated simultaneously with its protector, heparin.[38] Co-precipitation of an RNase inhibitor in our method is aiming to preserve integrity of RNA during its incorporation in $CaCO_3$ template and inside the capsule interior after template decomposition.

A vast majority of up to date publications on LbL assembled carriers of RNAs dials with siRNA payload. However, this seems to be a controversial choice at the current stage of research on intracellular fate of drug delivery systems. The observation elsewhere[36] warns that downregulation of many proteins could be a result of disturbance of the intracellular environment in response to stress caused by capsule uptake, but not a matter of gene silencing as it was expected. Indeed, although transfected human prostate carcinoma cells decreased the expression of targeted antiapoptotic protein, survivin, it was done with the same intensity as in response to uptake of empty capsules; and regardless of the presence or absence of the siRNA payload, the transfected cells also demonstrated decrease in the expression of other proteins with survivin-unrelated mRNA sequences. To be sure that the observed changes in protein expressions have no impact of a cellular stress response, luciferase mRNA was used in our transfection experiments. The choice of mRNA is also based on high importance of mRNA delivery for cell reprogramming purposes; thus, an effective and biologically safe mRNA delivery system will make a high impact to stem cell research and regenerative medicine.

2. Experimental Details

2.1. Reagents and materials

Chemicals dextran sulfate, sodium salt (DS, MW > 500 000), poly-L-arginine hydrochloride (PARG, MW > 70 000), tetramethylrhodamine isothiocyanate mixed isomers, calcium chloride, sodium hydrogen carbonate, sodium chloride, hydrochloric acid, ethylenediaminetetraacetic acid solution (EDTA), phosphate buffered saline (PBS) and boric acid obtained from Sigma-Aldrich and Hoechst stain obtained from Invitrogen were used without further purification. RNA-containing solutions were prepared using nuclease free water (Thermo Scientific) adding the Murine RNase inhibitor from New England Biolabs. PARG-tetramethylrhodamin isothiocyanate (PARG-TRITC) was synthesized in boric buffer pH 9 as described elsewhere.[39] HEK293T cells (ATCC) were cultured in Dulbecco's Modified Eagle Medium containing 15% of fetal bovine serum (15% FBS-DMEM) supplemented with 2 mM L-glutamine (all manufactured by Gibco). Deionized water with specific resistivity higher than 18.2 MΩcm from a three-stage Milli-Q Plus 185 purification system was used to prepare polymer and salt solutions. All salts and EDTA solution were autoclaved prior to be used for RNA encapsulation.

Sterile BD Falcon 24-well flat bottom cell culture plates (BD Bioscience) were used for $CaCO_3$ synthesis and RNA encapsulation. Polygon shaped 15mm × 6 mm magnetic stirring bar without pivot ring was obtained from Sigma-Aldrich. Single side polished boron-doped Prime silicon wafers (675 µm thick) were purchased from Syst Integration Pte Ltd. (Singapore).

2.2. Preparation of RNA

Total cellular RNA from HEK293T cells and mESCs was isolated using the TRIzol® Plus RNA Purification Kit from Life Technologies according to the manufacturer's instructions. Luciferase mRNA was synthesized with the MEGAscript T7 kit (Ambion), with 1.6 µg of purified tail PCR product to template each 40 µL reaction. A custom ribonucleoside blend was used comprising 3'-0-Me-m7G(5')ppp(5')G ARCA cap analog (New England Biolabs), adenosine triphosphate and guanosine triphosphate (USB), 5-methylcytidine triphosphate and pseudouridine triphosphate (TriLink Biotechnologies). Final nucleotide reaction concentrations were 6 mM for the cap analog, 1.5 mM for guanosine triphosphate, and 7.5 mM for the other nucleotides. Reactions were incubated for 3–6 h at 37°C and DNase treated as directed by the manufacturer. RNA was purified with Ambion MEGAclear spin columns, then treated with Antarctic Phosphatase (New England Biolabs) for 30 min at 37°C to remove residual 5'-triphosphates. Treated RNA was re-purified (Figure 1) and quantitated by Nanodrop (Thermo Scientific). Gel electrophoresis was carried out using Biorad PAC2000 on RNA samples diluted to 10 ng/mL with nuclease free water also containing RNase inhibitor at a 1:500 ratio.

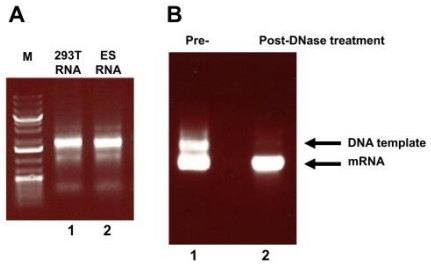

Figure 1. Preparation of RNAs. Total cellular RNA from HEK293T calls and ES cells (a). Luciferase mRNA reporter (b). Synthetic mRNA encoding luciferase was produced by in vitro transcription using T7 RNA polymerase from DNA template. Template was digested with DNase treatment (lane 2) to obtain pure mRNA.

2.3. Encapsulation of RNA

Incorporation of RNA in $CaCO_3$ microparticles were performed in the well of a sterile flat bottom 24-well cell culture plate by a co-precipitation method as shown in Figure 2. Each RNA, $CaCl_2$ and $NaHCO_3$ solution contained 1:100 volume part of RNase inhibitor.

In the first step, 0.5 mL of $CaCl_2$ solution (1 M) was added into the well of a just opened cell culture plate placed onto a magnet plate and aligned in a way that the operating well occurred in the centre of the magnet plate. Then a magnetic stirring bar was bottomed the well followed by adjusting the stirring speed to provide thorough mixing of solutions with no splashing. In the second step, 0.5 mL solution containing 100 ng of RNA and 0.5 mL of $NaHCO_3$ solution (1 M) were consequently added into the agitated $CaCl_2$.

The synthesized $CaCO_3$ microparticles containing RNA in their pores were washed with DI water via subsequent centrifugation/resuspension steps to remove residual salts from the medium. Multilayer shells were then assembled by immersing successively the $CaCO_3$/RNA microparticles in aqueous solutions of polyanion (dextran sulphate, DS) and polycation (poly arginine, PARG) for 10 min until 2 bi-layers were achieved ($[DS/PARG]_2$).

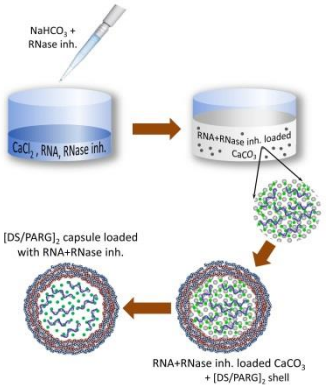

Figure 2. Schematic representation of encapsulation of RNA in $[DS/PARG]_2$ capsules while inhibiting activity of nucleases. At first, $CaCO_3$ is co-precipitated with a molecular cocktail of RNA and RNase inhibitor. Each RNA, $CaCl_2$ and $NaHCO_3$ solution contains 1:100 volume part of RNase inhibitor. Then the RNA-loaded $CaCO_3$ microparticles are used as a template for layer-by-layer assembly of two bi-layers of DS/PARG followed by the $CaCO_3$ decomposition.

Polymers used for capsule fabrication were dissolved in water in concentration of 2 mg/mL in the presence of 0.5 M NaCl and 1:500 volume part of the RNase inhibitor. After each deposition step, the RNA loaded core/shell microparticles were centrifuged. The supernatant was replaced with the pure water, and the particles were resuspended. The washing procedure was applied to ensure that no uncoupled polyelectrolyte remained in the sample. $CaCO_3$ template was then removed by EDTA treatment. For this purpose, multilayer coated $CaCO_3$/RNA microparticles were placed in 0.2 M EDTA buffer solution at pH 7.4 for 15 min, followed by two times of washing with water. Complete elimination of inorganic template was each time verified by observing the capsules under optical microscope. Supernatants obtained upon core dissolution and sample washings, were collected for further analysis of the RNA concentration.

2.4. RNA Concentration Measurements

RNA concentration in the stock solution and supernatants was measured by absorbance at 260 and 280 nm by the Nanodrop instrument. DI water was used as the reference. The amount of RNA loaded in the whole bunch of microcapsules was determined as the difference between the total amount of RNA used for $CaCO_3$ co-precipitation and the amount lost over shell assembly and core decomposition. For that purpose, RNA concentration was measured in the supernatant collected during each step of microcapsule fabrication. The cumulative loss of RNA was then deducted from the initial amount of RNA to give the amount of RNA contained in the bunch of microcapsules. Since the residual salts and polymer molecules can interfere with absorbance measurements, the RNA in the supernatant collected was extracted and redispersed before measuring the RNA concentration by Nanodrop.

2.5. Capsule Counting

Capsules were serially diluted at 10, 100, 1000, 10000 times in DI water in triplicates. The sample was put into round bottom 96 well plates. Number of capsules in each well was counted using LSR

Fortessa 96 high throughput sampler. Briefly, the liquid in each well was uniformly mixed and 50 µL was taken from each well. The total particle number was counted based on the gating set using forward and side scatter or by fluorescence intensity when the capsules were labelled. From the average count in triplicate wells and the serial dilution factor, the original concentration of the capsule was back calculated.

2.6. *In vitro* Cytotoxicity Studies

The fabricated capsules were pre-washed with DMEM and added into HEK293T cells cultured in 15% FBS-DMEM. Different doses of capsules were loaded on to cells. The growth of HEK293T cells was monitored over 48 h. The cell number at the end of 48 h was counted by hemocytometer or LSR Fortessa 96.

2.7. Microscopy

Scanning Electron Microscopy (SEM) was carried out in secondary electron imaging mode at 5 keV with JEOL FE SEM JSM-6700F electron microscope. 10 µL of either $CaCO_3$/RNA or RNA-loaded capsule suspensions in DI water were placed onto a silica wafer and dried at ambient conditions. Then a conductive coating was created by sputtering the wafer with gold for 20 s.

Confocal laser scanning microscopy (CLSM) images were captured with Olympus FluoView FV1000 (Olympus, Japan) laser scanning confocal microscope using a 100x/1.45 oil objective, with 543 nm HeNe laser as the excitation source. Brightfield and fluorescence images were captured using Axio Observer.Z1 (Zeiss, Germany) using 10×, 20× and 40× objective. Cellular uptake of capsules was visualized using Zeiss LSM 5 DUO inverted Laser Scanning Confocal Microscope. Images were taken with 60x magnification, 2× zoom, with pinhole size of 1 µm in z-series of 1 µm step size. Z-stack images were processed with LSM image browser (Zeiss).

3. Results and Discussion

3.1. Capsules with inhibited activity of RNases

Although RNA will be protected from environmental RNase contamination once absorbed by $CaCO_3$, it is essential to purify RNAs and encapsulate them in condition free of active RNases to preserve integrity during co-precipitation with $CaCO_3$, residence in the capsule interior after core decomposition, and intracellular delivery of RNA. In case of $CaCO_3$ – assisted encapsulation of unprotected luciferase mRNAs reporter, luciferase activity in the transfected cells was detected only for the batches of DNase untreated mRNAs probably as a result of DNA contamination. Gel electrophoreses revealed that the RNAs suffer a loss of integrity once added to either of calcium or sodium salt solution presumably because of the presence of RNases in these chemicals. After the RNase-inhibitor was introduced to salt solutions as it described in the Experimental section, total RNA incorporated in $CaCO_3$ was detected in intact form (Figure 3). To figure that out, $CaCO_3$ particles with incorporated RNA were dissolved with EDTA, and then RNA was separated by gel electrophoresis.

$CaCO_3$ template largely restricts mobility of incorporated molecules thus also protecting them from degradation by external agents during the process of multilayer shell assembly. To avoid degradation of those RNA molecules occur close to the interface, the RNase inhibitor was also added to the DS and PARG solutions used to form the capsule. Figure 4 displays $CaCO_3$ particles co-precipitated with RNA and RNase inhibitor as described above (Figure 4a) and the molecular-cocktail-loaded $[DS/PARG]_2$ capsules assembled on them (Figure 4b-d). The SEM and optical microscopy images reveal the templates and the corresponding capsules are successfully formed being 1 µm – 2 µm in diameter.

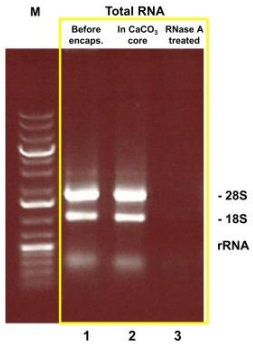

Figure 3. Quality check of RNA co-precipitated with $CaCO_3$ in the presence of RNase inhibitor. Lanes: 1. Purified total cellular RNA. 2. RNA consequently incorporated and released from $CaCO_3$ after $CaCO_3$ decomposition by EDTA. 3. #2 + RNase treatment.

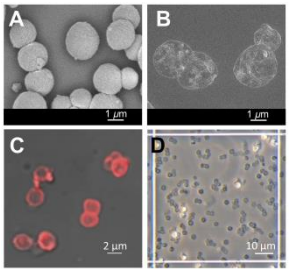

Figure 4. Successful fabrication of RNA-loaded capsules. SEM image of RNA-loaded $CaCO_3$ microparticles (a) and the corresponding $[DS/PARG]_2$ capsules (b). CLSM image of TRITC-PARG labeled capsules in H_2O (c). $[DS/PARG]_2$ capsules in 1×PBS on hemocytometer counting grid.

3.2. Loading efficiency

Concentration of mRNA from mouse ES cells was measured in the supernatant collected during each step of microcapsule fabrication and the total RNA lost was then subtracted from the initial amount of RNA (100 µg) to give the amount of RNA encapsulated in the microcapsules. A total loading efficiency of (39.9 ± 6.3) % was observed for RNA during PEM fabrication in our study. The trend for the cumulative loss of RNA at each step is presented in Figure 5, which suggests that the loss of RNA is greater in the polycation (PARG) solution compared to that in the polyanion (DS) solution. This could be because the polycation can couple RNA causing its release and hence the greater loss of RNA during polycation (PARG) layer formation. The loss of RNA is much smaller during the subsequent washing steps after the polymer bilayer has formed. Extraction of the $CaCO_3$ template by EDTA also caused burst release

of a major fraction of the incorporated RNA, which reduced after the washing step to almost negligible during the second wash. The overall efficiency of RNA encapsulation in the $[DS/PARG]_2$ capsules is within the error similar to that observed for FGF2 encapsulation in DS/PARG capsules comprising 5 bi-layers ((36.9 ± 4.2) %) or 7 bi-layers ((42.4 ± 4.6) %), and almost considerably higher than found for the 3 bi-layer thick capsules ((29.4 ± 5.0) %).[38]

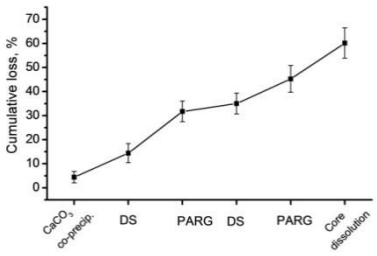

Figure 5. Cumulative loss of RNA during the $[DS/PARG]_2$ encapsulation process.

3.3. Capsule-cell interactions

The levels of cytotoxicity and internalization are the key parameters to be understood for *in vitro* application of capsules as delivery vectors. Since the first prove of their cellular uptake and biodegradability,[19] interactions of the 2 µm - 4 µm DS/PARG-based capsules with several cell lines were studied. These capsules were generally found to be well tolerated by cells. For instance, viability of L929 mouse fibroblast cells was ca 80% after exposure to 50 capsules/cell.[38] As for the internalization possibility, uptake and consequent complete degradation of capsules were observed for actively phagocyting dendritic cells.[40] Moreover, other cell lines, for instance, VERO,[19] L929 mouse fibroblast cells[38] and embryonic NIH/3T3 fibroblasts[41] were also shown to internalize and degrade DS/PARG-based capsules. Since there is no data available in literature specific to HEK293T cells, this cell line is examined here with the scope to assess viability in the presence of $[DS/PARG]_2$ capsules as well as the capsule internalization level.

For the viability studies, HEK293T cells were cultured for two days in the presence of hollow $[DS/PARG]_2$. As shown in Figure 6a, with the capsule densities less than 50 per cell, the growth of HEK293T cells was not significantly impaired over 48 h period. The observed level of viability is very similar to that previously reported for DS/PARG-based capsules and L929 mouse fibroblast cells.[38]

To monitor their uptake and intracellular distribution, the capsules were synthetized with the fluorescent PARG-TRITC as a positive charged polymer. Then HEK293T cells were transfected with these TRITC-labeled capsules at the densities of 5 and 50 capsules per cell and the number of cells with internalized capsules was measured by LSR Fortessa 96 after 48 h of incubation. Figure 6b clearly suggests the amount of cells with internalized capsules is in positive relation with the capsule density, however, even at the density of 50 capsules per cell, the level of internalization was measured quite low: ~23% of cells containing the $[DS/PARG]_2$ microcapsules.

The interaction of the $[DS/PARG]_2$ microcapsules with HEK293T cells was also examined by confocal microscope with z-stacks after

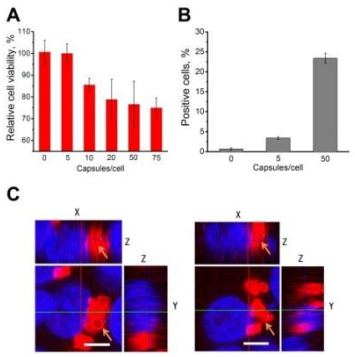

Figure 6. $[DS/PARG]_2$ capsule interaction with HEK293T cells: (A) Relative viability of HEK293T cells after 48 h of incubation with capsules at different capsules/cell ratio. (B) % of cells with internalized capsules after 48 h of incubation. (C) CLSM representative images showing the internalization of $[DS/PARG]_2$ capsules labelled with TRITC within HEK293T cells. After 48 h, the cells were washed and stained with Hoechst and imaged in z-stack (1 µm per step). For every inlet figure, the central square image shows a maximum projection on x-y direction, whereas the rectangular images at the side denote the reconstruction and maximum projection on the z direction (depth). Scale bar = 5 µm.

48 h of incubation at 50 capsules/cell. The cells were washed to remove the non-internalized capsules from the medium and stained with Hoechst to visualize their nucleoi. Figure 6c shows the 3D images clearly demonstrating cellular intake of capsules. The centre square shows x-y dimension of the 3D image, whereas the rectangular images at each side denote the reconstruction of the signal on the z direction along x or y side (the depth of the imaging). The capsules exhibit cytoplasmic localization as fluorescent signal are devoid in the nucleus but localize very close to the nucleoi of cells. More importantly, the close proximity of the capsule to the nucleoi and their localization at the same plane with the nucleoi on the z axis (Figure 6c, orange arrows) highly suggest their internalization into the cells instead of stayed on top of the confluent HEK293T cells sheet.

For quantitative assessment and optimization of RNA delivery, it is useful to develop RNA reporter system. For this purpose, we produced capped mRNA by *in vitro* transcription with T7 RNA polymerase (Figure 1b). These synthetic mRNAs were then encapsulated and delivered into HEK293T cells. Delivered mRNAs were successfully translated into luciferase protein as detected by luciferase enzyme activity in cell lysate. Relative activity of luciferase was meaningfully higher in the cells treated with mRNA encapsulated in $[DS/PARG]_2$ shells simultaneously with RNase inhibitor compare to those incubated with free mRNA or mRNA encapsulated alone (Figure 7). However, efficacies of commercially available delivery systems like lipofectamine loaded with the same amount of mRNA as used for co-precipitation with $CaCO_3$ were not matched by the capsules. Our estimations showed the capsules were 36-fold less efficient than lipofectamine. This could be an issue of different possibilities listed below. (I) The capsules were internalized by the cells, but their mRNA contents were not released into right compartment for translation. Further studies will

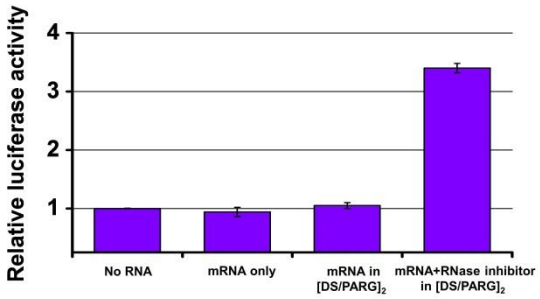

Figure 7. Delivery of luciferase mRNA reporter. Luciferase mRNA was encapsulated into $[DS/PARG]_2$ with or without RNase inhibitor and delivered into HEK293T cells. mRNA expression was checked by luciferase activity in cell lysate 16 h after delivery.

involve understanding of the capsule fate inside cells to determine the exact site of the mRNA release and tuning the release via changing the capsule shell constituents and the shell thickness.[42] (II) The capsules delivered too much functional mRNA into cell causing translational squelching. It is possible that large amount of introduced mRNA caused titration of translational machinery in the cells.[43] Although this result could indicate successful delivery of large amount of mRNA into living cells, it also invokes the detailed investigation of the delivery efficacy and optimal amount of mRNA to achieve whole transcriptome replacement. (III) Different total cargo loading efficiency and different level of cell internalization for the capsules and the liposomes. The efforts to increase the number of cells with internalized capsules are currently being made involving synthesis of sub-micrometre $CaCO_3$ template[44] and tackling the capsule aggregation issue.[45]

Conclusions

Layer-by-Layer (LbL) assembled capsules of dextran sulfate and poly-L-arginine have been successfully loaded with luciferase mRNA reporter via $CaCO_3$ microparticle-assistant preloading method. The encapsulation routine was elaborated to introduce RNase inhibitor in the capsule formulation so that the encapsulated genes remained protected over the loading and delivery process. Successful transfection proved by activity of luciferase detected in lysate of cells treated with capsules simultaneously loaded with mRNA and RNase inhibitor indicates reliability and good perspectives of the encapsulating method for delivery of different types of RNA. Both encapsulation and co-delivery with RNase inhibitor were shown critical for effective transfection, as no RNA expression was detected in the cells treated with free mRNAs and mRNAs encapsulated without RNase inhibitor.

Future research will attempt to improve transfection efficiency of the LbL capsules which will involve understanding and tuning of the mRNA intracellular release from the capsules and determination of the optimal amount of the delivered mRNA. The capsule penetration to non-actively phagocyting cells will be also improved. This might be achieved by reducing the size of the $CaCO_3$ co-precipitates and thus the size of the resulting capsules. Since smaller capsules are usually prone to aggregation, this issue will be carefully attended and tackled.

Acknowledgements

The study was supported by A*STAR's Joint Council Project Grant (Project No 1231AFG022).

Notes and references

1 K. Takahashi and S. Yamanaka, *Cell*, 2006, **126**, 663.
2 R. A. Stull and F. C. Szoka, *Pharm. Res.,* 1995, **12**, 465.
3 S. D. Patil, D. G., Rhodes and D. J. Burgess, *AAPS J.*, 2005, **7**, E61.
4 D. Putnam, *Nat. Mater.*, 2006, **5**, 439.
5 W. Walther, and U. Stein, *Drugs*, 2000, **60**, 249.
6 W. Wang, W. Li, N. Ma and G. Steinhoff, *Curr Pharm Biotechnol.*, 2013, **14**, 46.
7 K. H. Khan, *Asian J. Exp. Biol. Sci.*, 2010, **1**, 208.
8 J. A. Wolff and D. B. Rozema, *Mol. Ther.*, 2008, **16**, 8.
9 M. L. Bondi and E. F. Craparo, *Expert Opin. Drug Deliv.*, 2010, **7**, 7.
10 P. Chollet, M. C. Favrot, A. Hurbin and J. L. Coll, *J. Gene Med.*, 2002, **4**, 84.
11 J. D. Tousignant, A. L. Gates, L. A. Ingram, C. L. Johnson, J. B. Nietupski, S. H. Cheng, S. J. Eastman and R. K. Scheule, *Hum. Gene Ther.*, 2000, **11**, 2493.
12 M. N. Antipina, I. Schulze, M. Heinze, B. Dobner, A. Langner and G. Brezesinski, *Chem. Phys. Chem.*, 2009, **10**, 2471.
13 Y. Ping, D. C. Wu, J. N. Kumar, W. R. Cheng, C. L. Lay and Y. Liu, *Biomacromolecules*, 2013, **14**, 2083.
14 X. J. Loh, Z. X. Zhang, K. Y. Mya, Y. L. Wu, C. B. He and J. Li, *J. Mater. Chem.*, 2010, **20**, 10634.
15 X. Y. Lai, M. Agarwal, Y. M. Lvov, C. Pachpande, K. Varahramyan and F. A. Witzmann, *J. Appl. Toxicol.*, 2013, **33**, 1316.
16 N. Q. Jia, Q. Lian, H. B. Shen, C. Wang, X. Y. Li and Z. N. Yang, *Nano Lett.,* 2007, **7**, 2976.
17 H. Kim and W. J. Kim, *Small*, 2014, **10**, 117.
18 X. H. Liu, D. M. Ma, H. Tang, L. Tan, Q. J. Xie, Y. Y. Zhang, M. Ma and S. Z. Yao, *ACS Appl. Mater. Interfaces*, 2014, **6**, 8173.
19 B. G. De Geest, R. E. Vandenbroucke, A. M. Guenther, G. B. Sukhorukov, W. E. Hennink, N. N. Sanders, J. Demeester and S. C. De Smedt, *Adv. Mater.*, 2006, **18**, 1005.
20 M.N. Antipina, and G. B. Sukhorukov, *Adv. Drug Deliv. Rev.*, 2011, **63**, 716.
21 M. Delcea, H. Moehwald, and A. G. Skirtach, *Adv. Drug Del. Rev.*, 2011, **63**, 730.
22 M. N. Antipina, M. V. Kiryukhin, A. G. Skirtach and G. B. Sukhorukov, *Int. Mater. Rev.*, 2014, **59**, 224.
23 A. Elbakry, A. Zaky, R. Liebl, R. Rachel, A. Goepferich and M. Breunig, *Nano Lett*., 2009, **9**, 2059.
24 M. Y. Lee, S. J. Park, K. Park, K. S. Kim, H. Lee and S. K. Hahn, *ACS Nano*, 2011, **5**, 6138.
25 S. T. Guo, Y. Y. Huang, Q. A. Jiang, Y. Sun, L. D. Deng, Z. C. Liang, Q. A. Du, J. F. Xing, Y. L. Zhao, P. C. Wang, A. J. Dong and X. J. Liang, *ACS Nano*, 2010, **4**, 5505.
26 H. Jaganathan, S. Mitra, S. Srinivasan, B. Dave and B. Godin, *PLOS ONE*, 2014, **9**, e91986.
27 U. Reibetanz, C. Claus, E. Typlt, J. Hofmann and E. Donath, *Macromol. Biosci.*, 2006, **6**, 153.
28 T. Suma, K. Miyata, Y. Anraku, S. Watanabe, R. J. Christie, H. Takemoto, M. Shioyama, N. Gouda, T. Ishii, N. Nishiyama and K. Kataoka, *ACS Nano*, 2012, **6**, 6693.
29 J. Ramos and K. Rege, *Mol. Pharm.*, 2013, **10**, 4107.
30 D. G. Shchukin, A. A. Patel, G. B. Sukhorukov and Y. M. Lvov, *J Am Chem Soc.*, 2004, **126**, 3374.
31 H. Wu, Y. F. Shi, C. S. Huang, Y. Zhang, J. H. Wu, H. B. Shen and N. Q. Jia, *J. Biomater. Appl.*, 2014, **28**, 1180.

32 T. Borodina, E. Markvicheva, S. Kunizhev, H. Moehwald, G. B. Sukhorukov and O. Kreft, *Macromol. Rapid Commun.*, 2007, **28**, 1894.
33 X. R. Zhang, D. Chabot, Y. Sultan, C. Monreal and M. C. DeRosa, *ACS Appl. Mater. Interfaces*, 2013, **5**, 5500.
34 A. N. Zelikin, Q. Li and F. Caruso, *Angew. Chem. Int. Ed.*, 2006, **45**, 7743.
35 A. N. Zelikin, A. L. Becker, A. P. R. Johnston, K. L. Wark, F. Turatti and F. Caruso, *ACS Nano*, 2007, **1**, 63.
36 A. L. Becker, N. I. Orlotti, M. Folini, F. Cavalieri, A. N. Zelikin, A. P. Johnston, N. Zaffaroni and F. Caruso, *ACS Nano,* 2011, **5**, 1335.
37 L. Warren, P. D. Manos, T. Ahfeldt, Y. H. Loh, H. Li, F. Lau, W. Ebina, P. K. Mandal, Z. D. Smith, A. Meissner, G. Q. Daley, A. S. Brack, J. J. Collins, C. Cowan, T. M. Schlaeger and D. J. Rossi, *Cell Stem Cell*, 2007, **7**, 618.
38 Z. She, C. Wang, J. Li, G. B. Sukhorukov and M. N. Antipina, *Biomacromolecules*, 2012, **13**, 2174.
39 G. Ibarz, L. Daehne, E. Donath and H. Moehwald, *Adv. Mater.*, 2001, **13**, 1324.
40 S. De Koker, B. G. De Geest, S. K. Singh, R. De Rycke, T. Naessens, Y. Van Kooyk, J. Demeester, S. C. De Smedt and J. Grooten, *Angew. Chem. Int. Ed.*, 2009, **48**, 8485.
41 P. Rivera-Gil, S. De Koker, B. G. De Geest and W. J. Parak, *Nano Lett.*, 2009, **9**, 4398.
42 Z. She, M. N. Antipina, J. Li and G. B. Sukhorukov, Biomacromolecules, 2010, **11**, 1241.
43 G. Gill and M. Ptashne, *Nature*, **334**, 721.
44 B. V. Parakhonskiy, A. Haase, and R. Antolini, *Angew. Chemie Int. Ed.*, 2012, **51**, 1195.
45 N. Pargaonkar, Y. M. Lvov, N. Li, J. H. Steenekamp, M. M. de Villiers, *Pharm Res.*, 2005, **22**, 826.

Delivery of luciferase messenger RNA to HEK293T cells is successfully performed by polymer multilayer microcapsules co-encapsulating RNase inhibitor.